Attachment of Virus to Host Cell Surface upon Specific Binding to Membrane Receptors and Attachment Factors

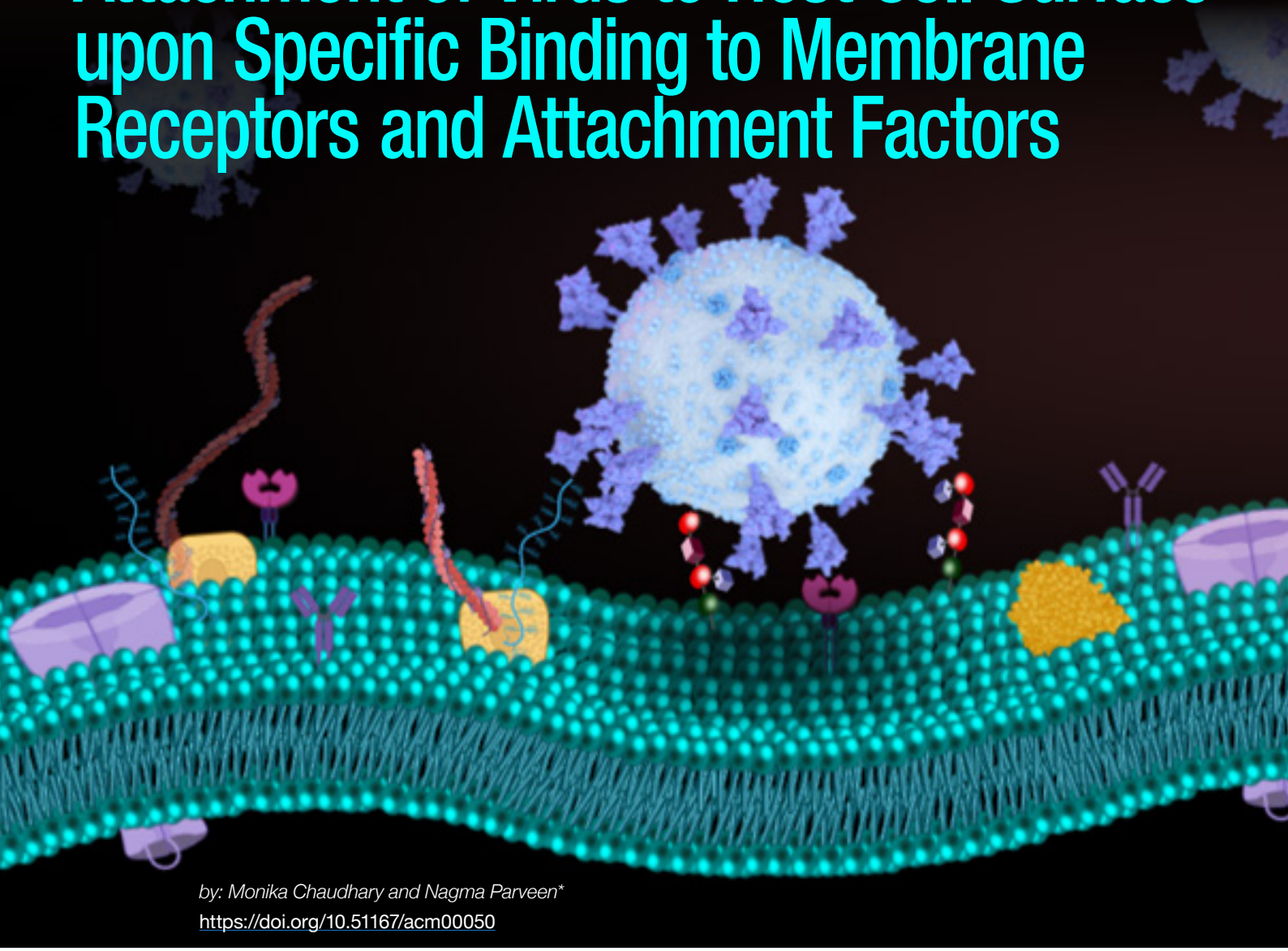

*by: Monika Chaudhary and Nagma Parveen**

https://doi.org/10.51167/acm00050

Introduction. Viruses are spherical particles of size 50–500 nm. The genome (DNA or RNA) of viruses is typically encapsulated by a protein shell, known as, capsid which is further coated by a protein-rich lipid bilayer for enveloped viruses. Most non-enveloped viruses have a rigid capsid with a high structural symmetry such as icosahedral, helical, and complex. The capsid and envelope proteins are part of the structural proteins of viruses and provide distinct structural features. A major function of these structural proteins is determining the binding of viruses to host cells and these structural proteins are the most exposed on the viral surface. While viruses are simple biological nanoparticles devoid of genetic machinery, they can replicate once they enter a host cell. This is a multistep process starting with the interaction of the viral surface proteins with specific molecules of a cell surface. It is well established that virus particles must evade or cross through the 1.5-μm-thick proteoglycan shield surrounding a cell to reach the plasma membrane of the cell. Viruses have evolved to interact with the proteoglycans and receptors of the plasma membrane to trigger signals for endocytosis or membrane fusion, processes essential for cellular entry (Figure 1). Despite the fact that viruses can intrude multiple tissues and organs of a host, the infection predominates in specific organs and cell types. This is determined by the specific interaction of the viral surface proteins with the proteoglycans and plasma membrane receptors.

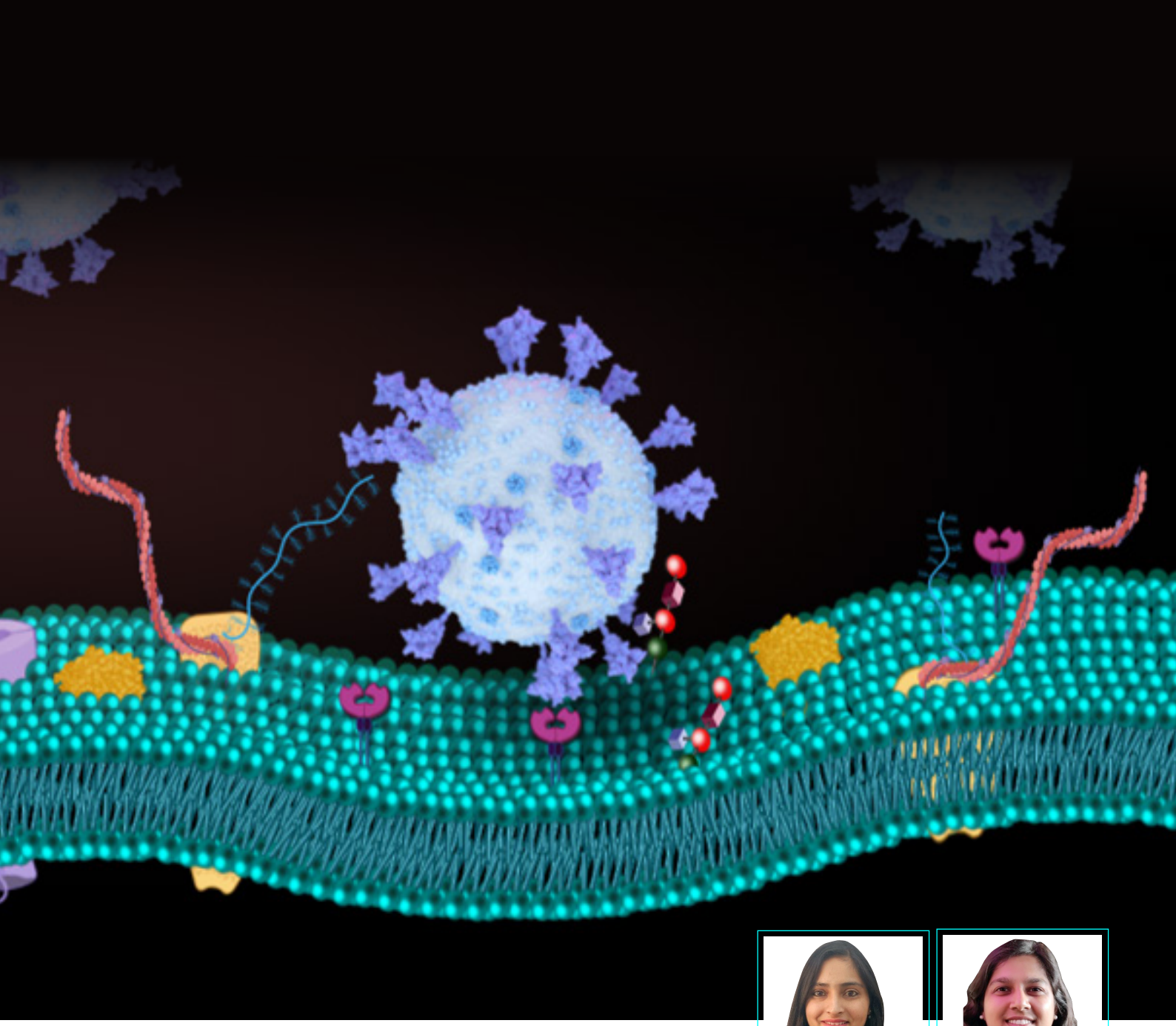

Molecular factors and interactions that determine the cellular attachment and entry of viruses.

The structure and configurational dynamics of the viral surface protein, receptors and glycans dictate their interactions. This is why resolving the receptor or glycan binding site of the viral proteins has been at the forefront of the virology and molecular biophysics of viruses. For example, the receptor binding domain (RBD) of the surface protein of human immunodeficiency virus (HIV-1) and severe acute respiratory syndrome coronavirus 2 (SARS-CoV-2) has been extensively studied in the literature. Both viruses bind to transmembrane proteins, i.e., CD4 and ACE2, respectively of the plasma membrane via protein-protein interactions.[1–4] The major surface protein of HIV-1 and SARS-CoV-2 is the envelope glycoprotein (Env) and the spike protein (S), respectively which protrudes out from the viral envelope by about 10 nm. Comparison of the structure of the Env and S proteins with and without complexation with the receptor has been the primary approach to analyse their RBD. The group of Subramaniam, Sodroski, Harrison, Veesler, McLellan, Tamm, Li, Munro, and Mothes have employed X-ray crystallography, cryo-electron microscopy, and single molecule Forster resonance energy transfer (smFRET) techniques to resolve the RBD, and interaction sites and even explored the configuration dynamic critical for the receptor binding[5–16] For example, the binding of the RBD of Env to CD4 triggers a conformational change of the different domains of Env (inner domain by 4 Å, bridging sheet by 10 Å and minor change in the outer domain by 2Å), enabling the binding of Env to a chemokine co-receptor (CCR5/ CXCR4). It has been confirmed

Monika Chaudhary

Dr. Monika Chaudhary completed her PhD degree in 2021 from IIT Ropar under the supervision of Dr. Narinder Singh and Dr. Kailash C. Jena. She was involved in studying the bulk phase and air/aqueous interfaces of nanomaterials along with their sensing applications in an aqueous medium. In 2022, she joined the research group of Dr. Nagma Parveen as a postdoctoral fellow in the Department of Chemistry at IIT Kanpur where she is exploring membrane-virus interactions. Her research interests are fluorescence microscopy, microfluidics devices for bioimaging and interfacial science.

Nagma Parveen

Dr. Nagma Parveen completed PhD in 2014 from the University of Muenster in Germany. She did postdocs at the Chalmers University of Technology, Sweden and the University of Leuven (KU Leuven), Belgium. She joined as an Assistant Professor in the Department of Chemistry, Indian Institute of Technology Kanpur in 2020. Her research interest is in the field of biophysics with a focus on understanding the early-replication cycle of viruses. Her lab is applying biomimetic platforms to probe the binding of intact virus particles to membrane receptors and attachment factors. Her research group employ fluorescence imaging and surface-sensitive analytical techniques such as SPR, QCM-D to evaluate the attachment-detachment kinetics and multivalent binding of viruses.

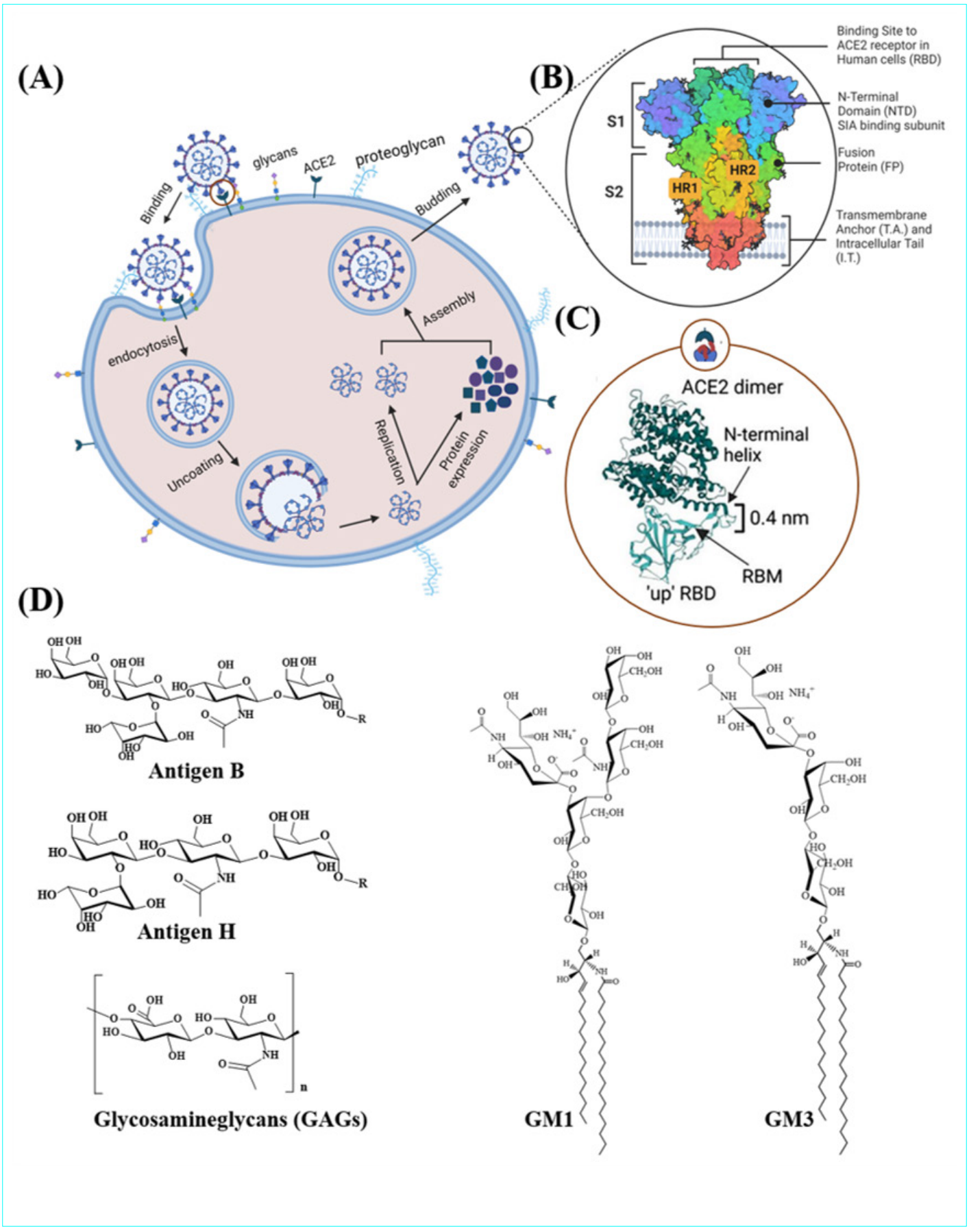

Figure 1. (A) Schematic diagram of SARS-CoV-2 attachment and replication in a host cell, (B) Structure of S protein along with its receptor binding sites, (C) Structure of the "up" RBD complexed with human ACE2 dimer (PDB ID: 6vw1, X-ray crystallography structure at 2.68 Å resolution (Lan et al. 2020; Shang et al. 2020). RBM: receptor binding motif and (D) Chemical structures of different glycans in host cell membranes.

that both the CD4 and chemokine co-receptor binding are essential for the cellular entry of HIV-1. The conformational changes of the S protein of SARS-CoV-2 have been a major topic of research since the beginning of the COVID-19 pandemic. The S protein of SARS-CoV-2 has up and down configurations. One or multiple RBDs are elevated by approximately 18 Å in the up configuration as measured by smFRET studies by Lu et al.[8]but real-time information that connects these structures is lacking. Here we apply single-molecule fluorescence (Förster, exposing the RBD for binding with the membrane receptors (Figures 1B and 1C). Cellular binding studies also indicate that the S protein of SARS-CoV-2 interacts with glycosaminoglycans (GAGs) such as heparan sulphate and heparin with a reasonably high affinity. Clausen et al. have shown that the S protein engages in cooperative binding with ACE2 in presence of GAGs[17]. These reports suggest SARS-CoV-2 may utilise cell surface GAGs as cellular attachment factors for an adequate cellular binding of the virus. The crystal structure of the RBD-receptor complexes of the viruses can indicate the potential number of H-bonds, salt bridges, Van der Waals interactions, electrostatic interactions and other interactions[18].

However, the interactions between the RBD and receptors in the solution phase depend on the hydrodynamics of the surrounding water, the configurational dynamics of the receptor and the viral protein, and so on. Therefore, a major area of research is tracing the kinetics and determining the thermodynamics of the receptor binding. Both ensemble-average and single-molecule techniques have been employed for this purpose. Quantitative parameters like binding enthalpy, energy, and equilibrium dissociation constant (k_D) determined from the corresponding experiments allow researchers to compare the receptor binding affinity in the soluble state or near-native environment, and often this binding energy deviates from the calculated/estimated energy from the structural analysis. This deviation becomes even more prominent during the binding of the intact virus to the receptors as multiple binding sites or viral proteins can engage in the interaction resulting in synergistic and multivalent interaction. Such type of binding has been rigorously explored for influenza viruses, in particular, influenza A viruses (IAVs).

The exact receptor of IAVs is not yet clear, but it is well-established that sialic acid is the attachment factor of these viruses. Sialic acid is abundant on the cell surface such as in branched chains of proteoglycans and exists in the form of glycolipids, and glycoproteins in the plasma membrane (chemical structure of a few given in Figure 1D).[19] The binding energy of the major surface protein of IAVs, i.e., hemagglutinin (HA) is relatively weak (k_D in millimolar) compared to the protein-receptor interaction in cases of HIV-1, SARS-CoV-2 and other viruses (k_D in nanomolar).[1,20–22] Moreover, IAVs contain another viral surface protein, neuraminidase (NA) which has the antagonistic function of HA[23]. The low receptor affinity of HA, the presence of HA and NA and their surface distribution results in the multivalent binding of IAVs on a cell surface. Single virus tracking has majorly contributed to the understanding of the dynamics of the multivalent binding of IAVs.[24–26] Even cooperative and/or synergistic binding of virus particles to membrane receptors of the same or different type can be explored upon imaging the binding kinetics and dynamics of viruses at a single particle level. Lee et. al., Mueller et. al., Sakai et al. and others have utilized single particle imaging with total internal reflection microscopy (TIRFM) to trace the binding kinetics and lateral mobility of IAV particles on biomimetic surfaces or artificial cell membranes such receptor-reconstituted supported lipid bilayers (SLBs)[24–28]. Liu et al. and Floyd et al. and others have analysed the fusion kinetics of IAVs on SLBs, in particular, the lipid mixing (hemifusion) and content mixing (fusion) using dual colour TIRFM imaging[29,30] The corresponding data indicates that the membrane hemifusion occurs upon configurational changes of 3 HA of IAVs. This means synergistic configurational changes of the viral protein are required for the successful fusion of intact IAV particles which might be also the case at the cellular level [15,29–31] These types of experimental studies allow researchers to pinpoint the molecular and membrane factors that are critical for the cellular entry of viruses. In our recent review article on the membrane attachment and fusion of HIV-1, IAVs and SARS-CoV-2, we have discussed case studies of the virus binding and fusion[32]. There we elaborate on how experiments using intact virus particles provide an improved understanding of the virus-receptor/attachment factor interaction and the process of membrane fusion.

Binding of human coronaviruses to glycans embedded in planar biomimetic membranes.

Our group aims to trace the real-time binding kinetics of virus particles to their membrane receptors and attachment factors at native or near-native conditions. The aim is to gain a fundamental understanding of the binding kinetics of intact virus particles and thereby, evaluate the influence of the multivalent, cooperative and/or synergistic binding in the observed kinetics. For this, we employ two types of membrane-based platforms, i.e., artificial SLBs and giant plasma membrane vesicles (GPMVs). We formulate SLBs by spreading lipid vesicles composed of synthetic or natural lipids on a planar surface. The receptors and attachment factors of viruses are reconstituted in the lipid vesicles and thereby, in SLBs. In this way, we formulate cell-membrane mimics with a controlled concentration and distribution of receptors and attachment factors. We trace the SLB formulation by acquiring time-lapse TIRF images of fluorescently labelled receptor-reconstituted vesicles and examine the kinetics of vesicles adsorption and rupturing and also, the growth kinetics of local bilayer patches upon the vesicle rupturing. The temporal changes in the number of accumulated vesicles (fluorescently labelled and with receptors) are plotted in Figure 2A and the inset schemes are shown to represent the stages of the SLB formations

These receptor-loaded SLBs are then used as cell membrane mimics and virus particles are injected either in the flow or non-flow conditions as shown in figure 2B. This type of experimental setup allows us to trace the attachment and detachment kinetics of intact virus particles to the receptors embedded in a membrane. We particularly developed a single particle imaging assay by fluorescently labelling the virus particles. In particular, we used wild-type human coronaviruses isolated from oro- and nasopharyngeal patient swabs and screened using SARS-CoV-2 specific primers. Viruses were cultured for samples having lower than 20 C_t values and then, the genome-inactivation of the virus sample was performed upon UV-light treatment. The replication-incompetent virus particles are labelled with a membrane-anchoring fluorophore. The labelled virus particles are imaged with the TIRF microscopy technique at a single particle level as shown in figure 2B. The key to single-particle imaging using the diffraction-limited TIRF microscopy technique is to perform homogeneous labelling of the virus particles and image the labelled viruses at a reasonably low particle concentration. With these two conditions, a sparse distribution of the labelled particles is achieved which allows spatial resolution of single virus particles upon TIRF imaging. Our lab is working to identify attachment factors other than ACE2 receptors which can substantially influence the membrane attachment of SARS-CoV-2. Thereby, we are probing a range of glycans with specific oligosaccharide sequences which can bind to SARS-CoV-2.

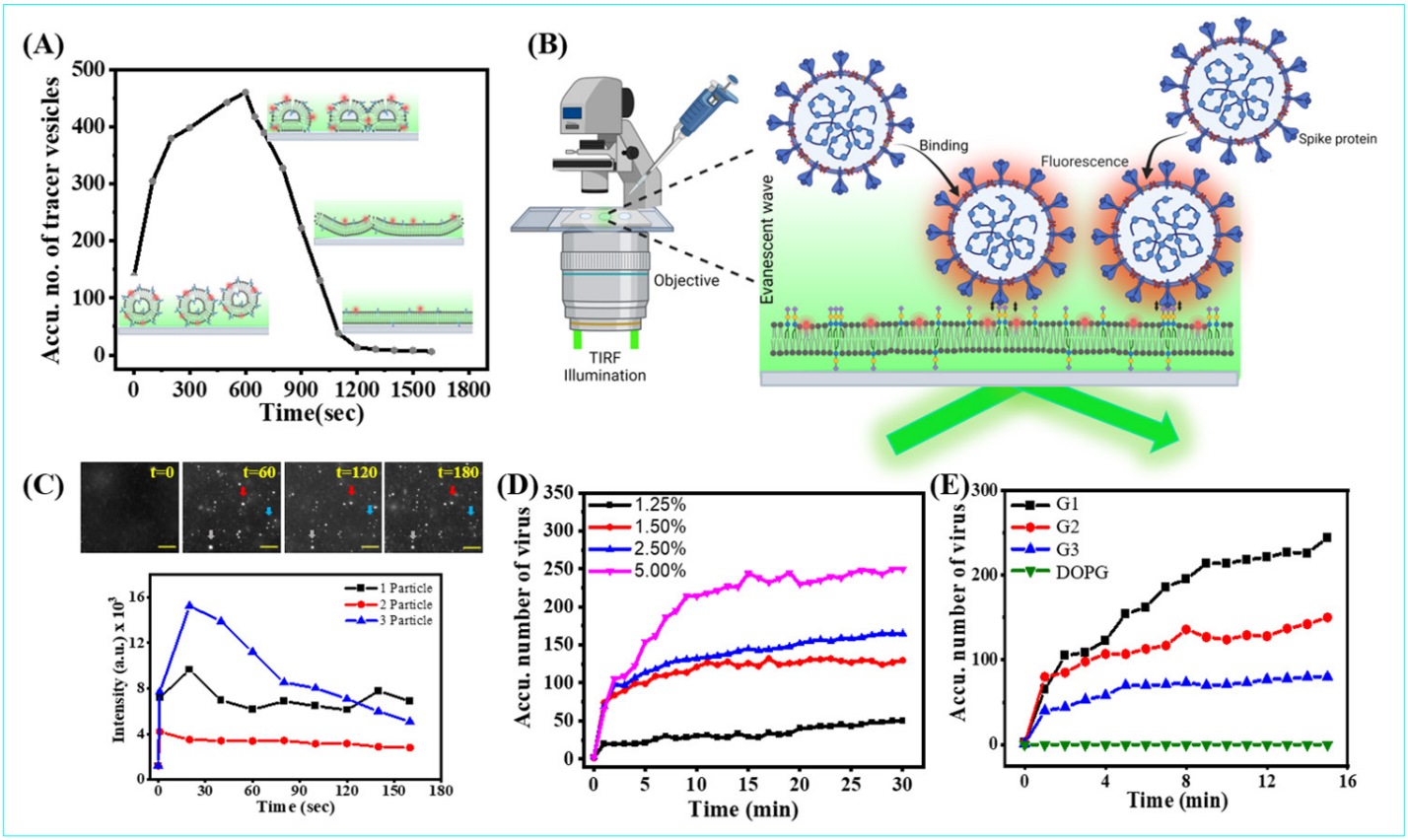

Figure 2. (A) Plot showing the accumulated number of tracer vesicles (vesicles of DOPC with 2.5 wt% G1) versus time along with the representation of vesicle attachment and rupture process. (B) Schematic representation of experimental setup of TIRF microscopy, (C) The micrographs of virus binding on SLB after 60 s, 120 s and 180 s along with the central pixel intensity of three virus particles (D) Line plot showing accumulated number of bound virus particles at different wt.% of G1 incorporated SLB versus time and (E) Plot between accumulated number of bound virus particles versus glycans G1, G2, G3 (5 wt. % of each in DOPC SLB) and pristine SLB after 15 mins. of attachment. Unpublished data of Negi and Sharma et al.

Our work is inspired by multiple recent reports indicating that the COVID-19 infection has a correlation with glycan expression. For example, Samuelsson et al. recently studied antibody induced inhibition of the RBD with human (HEK293T) and hamster cell lines (CHO-S and Lec3.2.8.1) and observed high antibody reactivity towards RBD produced with Lec3.2.8.1 cell line which is devoid of sialic acid expression[33] This report indicates that even slight modulation in the glycan content can impact the antibody activity which in turn means a significant role of glycans in the cellular infection caused by SARS-CoV-2. Many coronaviruses utilize glycan-binding for cellular attachment and entry, for example, a study by Park et al. demonstrates that the N-terminal domain (NTD) of the S protein of MERS-CoV binds with sialic acid on the cell surface[34]. As per their structural investigations, there is about 50-75Å distance between the receptor binding motif and the NTD. Computation analyses by Milanetti et al. show structural homology between the NTD of MERS-CoV and SARS-CoV-2 and both viruses can bind to glycan receptors of the host membrane via the NTD of the S protein[35]. A Recent study by Nguyen et al. confirmed the binding of S protein towards a series of synthetic oligosaccharides, gangliosides, and native N-glycans and reported a weak binding of the RBD with an average k_D > 200 μM[36]. Their cellular studies report that a decrease in the amount of sialic acid following any of these three different approaches, viz pharmacologically (via sialyltransferase (ST) inhibition), enzymatically (incubating with neuraminidase) and genetically (genetic elimination of SIA biosynthesis) in the ACE2 expressing cells results in decline RBD binding of SARS-CoV-2 pseudovirions. Hence, it is likely that SARS-CoV-2 is known to interact with cell surface glycans. Studies at a cellular and molecular level by Baker et al., Fantini et al., Petijean et al. and others show that indeed the S protein of SARS-CoV-2 can bind to cell surface glycans.[37–39] Computational and molecular docking data by Fantini et al. and Baker et al. confirm that glycans of specific sequence can bind to the NTD of the S protein of SARS-CoV-2 and the planar tip at the NTD docks perfectly with the sialic acid receptors on membrane.[37,39] In early 2022, Petijean et al. reported the binding dynamics of the S protein as well as intact SARS-CoV-2 particle with O-acetyl-sialic acid derivatives using single molecule force spectroscopy technique both *in-vitro* and at cellular level [38]. The authors showed that the S protein has a binding affinity (k_D) of 5.7 ± 5 μM and the virus particles achieve a multivalent binding with the sialic acid.

In our virus binding experiments, we acquired time-lapse images of labelled virus particles as they bind to the glycan-rich SLBs. As soon as the virus particles approach the surface and reach within the evanescent field of the TIRF illumination, we detect a fluorescence signal from the virus particles. The binding of virus particles to the SLBs can be seen from the steady fluorescence signal from the particles as measured over time. An intensity trace of a single virus particle upon its binding to the SLB is shown in Figure 2C. This type of particle intensity trace was observed more in numbers with an increased glycan concentration in SLBs and only a few non-specific binding events were detected in the absence of any glycan in SLBs (using pure zwitterionic or charged

phospholipid SLBs). We explored the virus binding for three different glycans which differ in their oligosaccharide sequence, in particular, combinations of sialic acid and galactose were used as the terminal sugar units in the glycans namely G1, G2 and G3. We implemented a single particle localization algorithm to detect single particles bound to an SLB and plotted the number of accumulated virus particles with time (Figure 2D). The corresponding data show number of the accumulated viruses on glycan-rich SLBs increases with glycan concentration in a non-linear manner (Figure 2E). We observed that with increasing the glycan availability in SLBs the rate constant of virus attachment (k_{on}) increases. The calculation of k_{on} was carried out by measuring the slope of virus binding for initial 30 seconds through a linear fitting. The molecular structure of glycans influence this concentration depended binding of virus particles as we observed a strong non-linear dependence on G1 and G2 over G3. An enzymatic cleavage of the terminal sialic acid from the glycans lowers the number of the virus binding events, indicating the terminal sialic acid of the glycans are critical in the virus attachment to the glycan-rich SLBs. In general, the virus particles bound to SLBs show weak lateral mobility at low glycan concentrations. This was not the case at higher glycan concentrations in SLBs, indicating multivalent binding of the virus with the membrane-embedded glycans. A similar multivalent binding of SARS-CoV-2 to the cell surface glycans has also been reported by Petijean et al[38].

Binding of human coronaviruses to receptors of isolated plasma membrane.

The application of artificial membranes like SLBs for virus binding studies have some limitations and among the major one is the compositional simplicity as compared to the plasma membrane. In general, cell membranes are crowded with transmembrane glycoproteins, glycolipids, sphingolipids, cholesterol and so on. Their lateral and interleaflet distribution and specific orientation in the membrane are not easy to mimic in receptor-reconstituted SLBs. A better membrane mimicking system will be if the plasma membrane is isolated directly from cells and this isolated membrane either in the form of vesicles or SLBs can be applied for virus binding experiments. In this line, we are working on isolating GPMVs upon chemical treatment of adherent mammalian cells. Mass spectrometry and functional studies using antibody-specific binding confirm that GPMVs retain the native composition of the plasma membrane while lacking the cytoskeleton[40–42]. A major difference between GPMVs and the plasma membrane of a cell is the membrane phase separation behavior. Lipid-disorder to order phase transition is observed upon lowering the temperature of GPMV but not for the plasma membrane of cells. It is

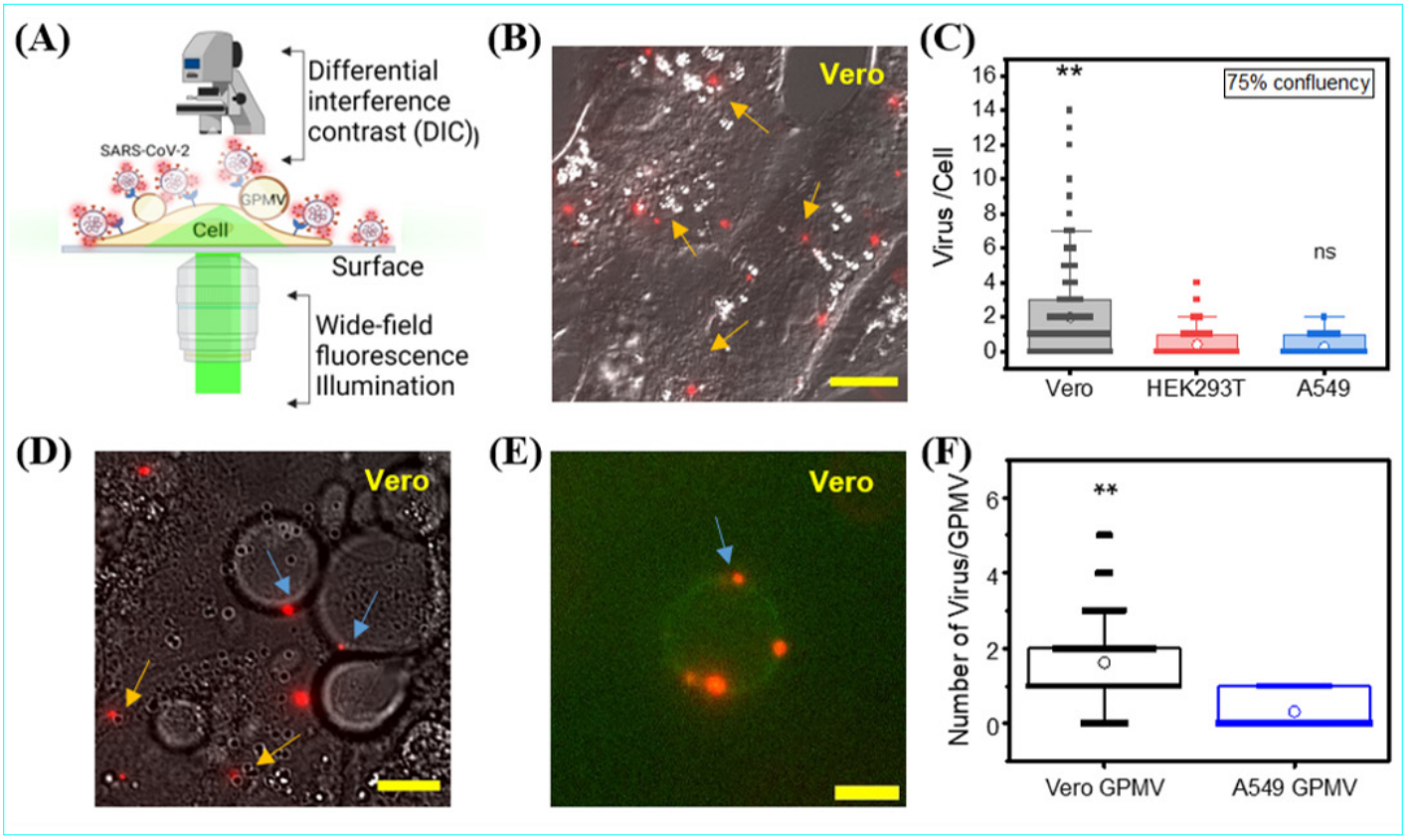

Figure 3. (A) Scheme of the microscopy set up illustrating DIC and wide-field epifluorescence imaging of viruses bound to cell attached GPMVs (drawn using Biorender.com), (B) Overlay of the DIC and fluorescence micrograph to show the binding of labelled viruses to the Vero cells. (C) Scatter plot of the number of bound viruses per cell at 75% cellular confluency. The distribution plot is analysed for >200 cells of each type. Significance of difference from the HEK293T data as control was assessed by one-sample t test; ns = not significant; *p < 0.02; **p < 0.001. (D) Overlay micrograph to show the binding of DiI-labelled viruses to the GPMVs and cell, (E) Dual-colour fluorescence micrographs showing DiI-labeled SARS-CoV-2 particles bound to a DiO-labelled cell-free GPMV derived from Vero cells, (F) Scatter plot of the number of bound virus particles per GPMV as determined from the acquired dual-color fluorescnce images. A total of 155 GPMVs were analyzed for each cell lines. Significance of difference from the A549 data as control was assessed by an one-sample t test; **p < 0.001. Yellow and blue arrows in (B), (D) and (E) are to indicate the binding of single viruses on the cell surface and on the boundary of GPMVs. Scale bars of fig B, D and E are 10, 10 and 5μm respectively. Unpublished data of Dey and Dhanawat et al.

hypothesized that the chemical treatment of cells induces an inter-leaflet reorganization of the membrane components which enables the formation of macroscopic lipid-order phases unlike microscopic lipid-rafts of the plasma membrane. This aspect is not yet fully explored. Group of Susan Daniel, Raya Sorkin, Marta Bally and Lukas Tamm have shown the applications of GPMVs or plasma membrane derived vesicles for studying membrane attachment and fusion of viruses[15,27,43–46]HIV must first fuse its lipid envelope with the host cell plasma membrane. Whereas the process of HIV membrane fusion can be tracked by fluorescence microscopy, the 3D configuration of proteins and lipids at intermediate steps can only be resolved with cryo-electron tomography (cryoET. In recent years, diverse groups have shown the application of such native vesicles for capturing or neutralizing viruses such as SARS-CoV-2, HIV-1 etc[15,27,43,45]HIV must first fuse its lipid envelope with the host cell plasma membrane. Whereas the process of HIV membrane fusion can be tracked by fluorescence microscopy, the 3D configuration of proteins and lipids at intermediate steps can only be resolved with cryo-electron tomography (cryoET. This indicates GPMVs can be used a membrane platform for virus binding.

We are working on formulating GPMVs from a range of adherent mammalian cells with varied levels of ACE2 expression. It is well-established that ACE2 is the primary receptor of SARS-CoV-2 and thereby, we aim at examining whether the receptor expression influence the virus binding to cells as well as GPMVs extracted from the cells. For this, we used three different adherent mammalian cell lines, i.e., Vero, HEK293T and A549. These cell lines have a different level of native ACE2 expression as confirmed by Western blotting. We compared the binding of SARS-CoV-2 to these cells by imaging the fluorescently labelled virus particles bound to the cell surface. For this, we coupled epifluorescence (widefield illumination) and brightfield imaging, and acquired fluorescence images of cell-bound virus particles and DIC images of the cells within the same region of interest (experimental setup shown in Figure 3A). These images were acquired in a subsequent manner and overlaid to visualize the virus localization on the cells (Figure 3B). We observed that the number of virus particles bound per cell has a statistically significant descending order as Vero > HEK293T > A549 as shown in Figure 3C. This is matching with the extent of ACE2 expression in these cell lines. We treated these cells with 25 mM paraformaldehyde (PFA) and 2 mM dithiothreitol (DTT) to induce vesiculation of the plasma membrane and detected vesicle protrusion from the plasma membrane. The vesicles grow up to 10 µm and release in the form of spherical GPMVs in the solution phase. We developed a virus binding assay to both cell-attached GPMVs and cell-free GPMVs employing either dual-color imaging or a combination of fluorescence and differential interference contrast (DIC) imaging. Figure 3D shows the overlay image of the fluorescence image and DIC image of virus particles bound to cell-attached GPMVs and Fig 3E shows a dual-color fluorescence image of virus particles bound to a free GPMV adsorbed on a polymer-coated cover glass. The number of bound viruses per GPMV shows the same trend as for the virus binding to the respective cell lines, indicating the receptors are functional in GPMV even upon the chemical treatment and virus particles can engage in binding with the outer membrane of GPMVs. Our analysis shows that an average of 3 and 2 virus particles bind per Vero and Vero-derived GPMVs. Cell free GPMVs derived from Vero cells show higher attachment of viruses per cell as compared to GPMVs derived from A549 cells as shown in Figure 3F, which is consistent with their respective ACE2 expression.

Outlook

It is of fundamental interest how viruses utilize their surface proteins to navigate the crowded cell surface, achieve attachment to the plasma membrane, and commence cellular entry. Resolving the molecules essential for these steps and understanding the molecular mechanism and cellular pathways are essential for designing antiviral drugs. The targets of the designed drugs are either the proteins on the virus surface or the virus-membrane interaction sites, impairing the cellular attachment and entry of viruses. While targeting the viral protein might appear a better approach, there are certain challenges in virus neutralization: 1) a high concentration of inhibitor or multivalent inhibitor is required to neutralize a relatively large number of surface proteins of viruses and 2) mutation of the viral protein may evade the neutralization. Irrespective of these challenges, monoclonal antibodies targeting the RBD have been successful in antiviral therapy and peptides have been used to block the configurational change of viral fusion protein essential for the membrane fusion[11,46–48] The other approach, i.e., inhibiting virus-membrane interaction has also been successful and several small molecule antiviral drugs are in the market. For example, Maraviroc is a clinically approved HIV-1 drug and it inhibits the virus interaction with the cellular chemokine co-receptor49. Another example is neuraminidase inhibitors such as zanamivir and oseltamivir which are used for the treatment of flu caused by IAVs50. Earlier it was thought of that these drugs impede the detachment of progeny IAVs. More recent studies are reporting that the viral neuraminidase is critical in the multivalent attachment of the virus and thus, the drugs are likely to affect the adequate membrane attachment of IAVs. The SLB and GPMV platforms we designed to study the virus-glycan and virus-receptor interaction membrane are applicable for screening the in-vitro inhibition efficacy of drug candidates. Any perturbation in the virus attachment-detachment kinetics or lateral dynamic of virus particles on these platforms can indicate the effect of drug candidates and the mode of inhibition. Moreover, well-established biophysical and analytical techniques like fluorescence imaging, and surface plasmon resonance can be employed to trace the binding kinetics. Therefore, glycan/receptor reconstituted SLBs and GPMVs are suitable membrane models to study the fundamentals of virus attachment to host cell surfaces and further, explore the inhibition effect by drug candidates.

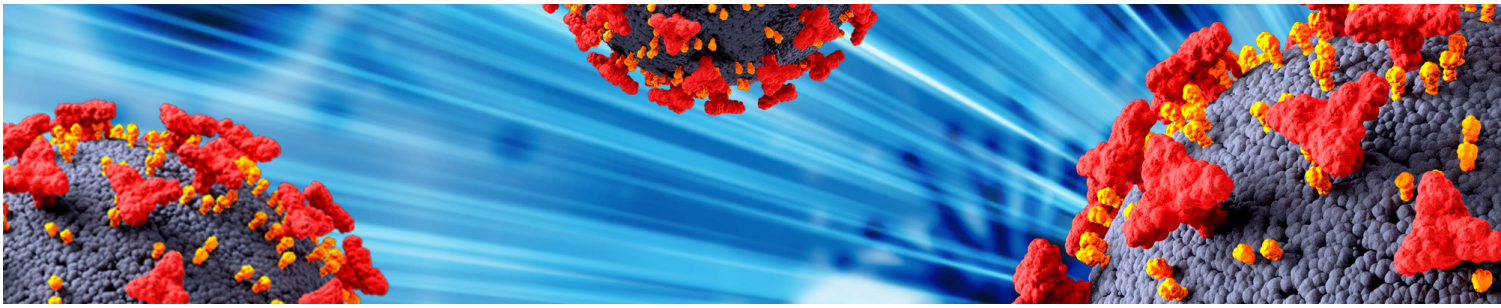

References:

1. Myszka, D. G. *et al.* Energetics of the HIV gp120-CD4 binding reaction. *Proc. Natl. Acad. Sci. U. S. A.* **97**, 9026–9031 (2000).
2. Clapham, P. R. & McKnight, Á. HIV-1 receptors and cell tropism. *Br. Med. Bull.* **58**, 43–59 (2001).
3. Shang, J. *et al.* Cell entry mechanisms of SARS-CoV-2. *Proc. Natl. Acad. Sci. U. S. A.* **117**, (2020).
4. Zhou, P. *et al.* A pneumonia outbreak associated with a new coronavirus of probable bat origin. *Nature* **579**, 270–273 (2020).
5. Merk, A. & Subramaniam, S. HIV-1 envelope glycoprotein structure. *Curr. Opin. Struct. Biol.* **23**, 268–276 (2013).
6. Liu, J., Bartesaghi, A., Borgnia, M. J., Sapiro, G. & Subramaniam, S. Molecular architecture of native HIV-1 gp120 trimers. *Nature* **455**, 109–113 (2008).
7. Das, D. K. *et al.* Direct Visualization of the Conformational Dynamics of Single Influenza Hemagglutinin Trimers. *Cell* **174**, 926-937.e12 (2018).
8. Lu, M. *et al.* Real-Time Conformational Dynamics of SARS-CoV-2 Spikes on Virus Particles. *Cell Host Microbe* **28**, 880-891.e8 (2020).
9. Mao, Y. *et al.* Molecular architecture of the uncleaved HIV-1 envelope glycoprotein trimer. *Proc. Natl. Acad. Sci. U. S. A.* **110**, 12438–12443 (2013).
10. Weis, W. I., Brünger, A. T., Skehel, J. J. & Wiley, D. C. Refinement of the influenza virus hemagglutinin by simulated annealing. *J. Mol. Biol.* **212**, 737–761 (1990).
11. Harris, A. K. *et al.* Structure and accessibility of HA trimers on intact 2009 H1N1 pandemic influenza virus to stem region-specific neutralizing antibodies. *Proc. Natl. Acad. Sci. U. S. A.* **110**, 4592–4597 (2013).
12. Wrapp, D. *et al.* Cryo-EM structure of the 2019-nCoV spike in the prefusion conformation. *Science (80-.).* **367**, 1260–1263 (2020).
13. Walls, A. C. *et al.* Structure, Function, and Antigenicity of the SARS-CoV-2 Spike Glycoprotein. *Cell* **181**, 281-292.e6 (2020).
14. Walls, A. C. *et al.* Cryo-electron microscopy structure of a coronavirus spike glycoprotein trimer. *Nature* **531**, 114–117 (2016).
15. Ward, A. E. *et al.* HIV-cell membrane fusion intermediates are restricted by Serincs as revealed by cryo-electron and TIRF microscopy. *J. Biol. Chem.* **295**, 15183–15195 (2020).
16. Shang, J. *et al.* Structural basis of receptor recognition by SARS-CoV-2. *Nature* **581**, 221–224 (2020).
17. Clausen, T. M. *et al.* SARS-CoV-2 Infection Depends on Cellular Heparan Sulfate and ACE2. *Cell* **183**, 1043-1057.e15 (2020).
18. Lan, J. *et al.* Structure of the SARS-CoV-2 spike receptor-binding domain bound to the ACE2 receptor. *Nature* **581**, 215–220 (2020).
19. Matrosovich, M., Herrler, G. & Klenk, H. D. Sialic Acid Receptors of Viruses. in *SialoGlyco chemistry and biology II* vol. 367 1–28 (Springer-Verlag Berlin Heidelberg, 2013).
20. Fei, Y. *et al.* Characterization of receptor binding profiles of influenza a viruses using an ellipsometry-based label-free glycan microarray assay platform. *Biomolecules* **5**, 1480–1498 (2015).
21. Xiong, X. *et al.* Receptor binding by a ferret-transmissible H5 avian influenza virus. *Nature* **497**, 392–396 (2013).
22. Yang, J. *et al.* Molecular interaction and inhibition of SARS-CoV-2 binding to the ACE2 receptor. *Nat. Commun.* **11**, 4541 (2020).
23. Byrd-Leotis, L., Cummings, R. D. & Steinhauer, D. A. The interplay between the host receptor and influenza virus hemagglutinin and neuraminidase. *Int. J. Mol. Sci.* **18**, 1541 (2017).
24. Sakai, T., Nishimura, S. I., Naito, T. & Saito, M. Influenza A virus hemagglutinin and neuraminidase act as novel motile machinery. *Sci. Rep.* **7**, 1–11 (2017).
25. Müller, M., Lauster, D., Wildenauer, H. H. K., Herrmann, A. & Block, S. Mobility-Based Quantification of Multivalent Virus-Receptor Interactions: New Insights into Influenza A Virus Binding Mode. *Nano Lett.* **19**, 1875–1882 (2019).
26. Lee, D. W., Hsu, H., Bacon, K. B. & Daniel, S. Image Restoration and Analysis of Influenza Virions Binding to Membrane Receptors Reveal Adhesion-StrengtheningKinetics. *PLoS One* **11**, e0163437 (2016).
27. Peerboom, N. *et al.* Cell Membrane Derived Platform to Study Virus Binding Kinetics and Diffusion with Single Particle Sensitivity. *ACS Infect. Dis.* **4**, 944–953 (2018).
28. Bally, M. *et al.* Physicochemical tools for studying virus interactions with targeted cell membranes in a molecular and spatiotemporally resolved context. *Anal. Bioanal. Chem.* **413**, 7157–7178 (2021).
29. Liu, K. N. & Boxer, S. G. Single-virus content-mixing assay reveals cholesterol-enhanced influenza membrane fusion efficiency. *Biophys. J.* **120**, 4832–4841 (2021).
30. Floyd, D. L., Ragains, J. R., Skehel, J. J., Harrison, S. C. & Van Oijen, A. M. Single-particle kinetics of influenza virus membrane fusion. *Proc. Natl. Acad. Sci. U. S. A.* **105**, 15382–15387 (2008).
31. Sieczkarski, S. B. & Whittaker, G. R. Influenza Virus Can Enter and Infect Cells in the Absence of Clathrin-Mediated Endocytosis. *J. Virol.* **76**, 10455–10464 (2002).
32. Negi, G., Sharma, A., Dey, M., Dhanawat, G. & Parveen, N. Membrane attachment and fusion of HIV - 1 , influenza A , and SARS - CoV - 2 : resolving the mechanisms with biophysical methods. *Biophys. Rev.* **14**, 1109–1140 (2022).
33. Samuelsson, E. *et al.* Sialic Acid and Fucose Residues on the SARS-CoV-2 Receptor-Binding Domain Modulate IgG Antibody Reactivity. *ACS Infect. Dis.* **8**, 1883–1893 (2022).
34. Park, Y. J. *et al.* Structures of MERS-CoV spike glycoprotein in complex with sialoside attachment receptors. *Nat. Struct. Mol. Biol.* **26**, 1151–1157 (2019).
35. Milanetti, E. *et al.* In-Silico Evidence for a Two Receptor Based Strategy of SARS-CoV-2. *Front. Mol. Biosci.* **8**, 1–11 (2021).
36. Nguyen, L. *et al.* Sialic acid-containing glycolipids mediate binding and viral entry of SARS-CoV-2. *Nat. Chem. Biol.* **18**, 81–90 (2022).
37. Baker, A. N. *et al.* The SARS-COV-2 Spike Protein Binds Sialic Acids and Enables Rapid Detection in a Lateral Flow Point of Care Diagnostic Device. *ACS Cent. Sci.* **6**, 2046–2052 (2020).
38. Petitjean, S. J. L. *et al.* Multivalent 9-O-Acetylated-sialic acid glycoclusters as potent inhibitors for SARS-CoV-2 infection. *Nat. Commun.* **13**, 1–12 (2022).
39. Fantini, J., Di, C., Chahinian, H. & Yahi, N. Structural and molecular modelling studies reveal a new mechanism of action of chloroquine and hydroxychloroquine against SARS-CoV-2 infection. *Int. J. Antimicrob. Agents* **55**, 105960–105969 (2020).
40. Keller, H., Lorizate, M. & Schwille, P. PI(4,5) P2 Degradation Promotes the Formation of Cytoskeleton-Free Model Membrane Systems. *ChemPhysChem* **10**, 2805–2812 (2009).
41. Sengupta, P., Hammond, A., Holowka, D. & Baird, B. Structural determinants for partitioning of lipids and proteins between coexisting fluid phases in giant plasma membrane vesicles. *Biochim. Biophys. Acta - Biomembr.* **1778**, 20–32 (2008).
42. Baumgart, T. *et al.* Large-scale fluid/fluid phase separation of proteins and lipids in giant plasma membrane vesicles. *Proc. Natl. Acad. Sci. U. S. A.* **104**, 3165–3170 (2007).
43. Yang, S. T. *et al.* HIV virions sense plasma membrane heterogeneity for cell entry. *Sci. Adv.* **3**, 1–13 (2017).
44. Costello, D. A., Hsia, C. Y., Millet, J. K., Porri, T. & Daniel, S. Membrane fusion-competent virus-like proteoliposomes and proteinaceous supported bilayers made directly from cell plasma membranes. *Langmuir* **29**, 6409–6419 (2013).
45. Cheppali, S. K., Dharan, R., Katzenelson, R. & Sorkin, R. Supported Natural Membranes on Microspheres for Protein–Protein Interaction Studies. *ACS Appl. Mater. Interfaces* **14**, 49532–49541 (2022).
46. Costello, D. A., Millet, J. K., Hsia, C., Whittaker, G. R. & Daniel, S. Single particle assay of coronavirus membrane fusion with proteinaceous receptor-embedded supported bilayers. *Biomaterials* **34**, 7895–7904 (2013).
47. Kwong, P. D. *et al.* Structure of an HIV gp120 envelope glycoprotein in complex with the CD4 receptor and a neutralizing human antibody. *Nature* **393**, 648–659 (1998).
48. Caillat, C. *et al.* Structure of hiv-1 gp41 with its membrane anchors targeted by neutralizing antibodies. *Elife* **10**, 1–26 (2021).
49. De Clercq, E. & Li, G. Approved antiviral drugs over the past 50 years. *Clin. Microbiol. Rev.* **29**, 695–747 (2016).
50. Bai, Y., Jones, J. C., Wong, S. S. & Zanin, M. Antivirals targeting the surface glycoproteins of influenza virus: Mechanisms of action and resistance. *Viruses* **13**, 1–16 (2021).